Biomolecules and Biomedicine
ISSN: 2831-0896 (Print) | ISSN: 2831-090X (Online)
Journal Impact Factor® (2022): 3.4
CiteScore® (2022): 5.3
www.biomolbiomed.com | blog.biomolbiomed.com

RESEARCH ARTICLE

TRANSLATIONAL AND CLINICAL RESEARCH

Unraveling the role of *LDHA* and *VEGFA* in oxidative stress: A pathway to therapeutic interventions in cerebral aneurysms

Jiaying Wu[1#], Lixia Lu[2#], Beibei Dai[3]*, and Aiyong Yu[1]*

[1]Department of Neurology, Songjiang Hospital Affiliated to Shanghai Jiao Tong University School of Medicine, Shanghai, China.

[2]Department of Neurology, Qingpu Branch of Zhongshan Hospital, Fudan University, Shanghai, China.

[3]Department of Ultrasound, Obstetrics and Gynecology Hospital of Fudan University, Shanghai, China.

***Corresponding authors:** Beibei Dai; Email: daibeibei.0823@163.com; Aiyong Yu; Email: aiyong07@sohu.com.

Associate editor: Masaru Tanaka

[#]These authors contributed equally to this work.

DOI: https://doi.org/10.17305/bb.2024.10510

Submitted: 22 March 2024/ **Accepted:** 22 May 2024/ **Published online:** 01 June 2024

Conflicts of interest: Authors declare no conflicts of interest.

Funding: Authors received no specific funding for this work.

ABSTRACT

Cerebral aneurysms (CA) are critical conditions often associated with oxidative stress in vascular endothelial cells (VECs). The enzyme lactate dehydrogenase A (LDHA) plays a crucial role in glycolysis and lactate metabolism, processes implicated in the pathogenesis of aneurysms. Understanding these molecular mechanisms can inform the development of novel therapeutic targets. This study investigated the role of lactate metabolism and lactate-related genes, particularly *LDHA* and vascular endothelial growth factor A (*VEGFA*) genes, in VECs during oxidative stress. Using the GSE26969 dataset, we identified differential expression of lactate-related genes and performed functional enrichment analysis, revealing significant associations with glycolysis and lactate metabolic pathways. To induce oxidative stress, VECs were treated with H_2O_2, and the expression of *LDHA* and *VEGFA* was analyzed using quantitative real-time polymerase chain reaction (qRT-PCR) and western blotting (WB) assays. Under oxygen-glucose deprivation/reperfusion (OGD/R) conditions, the effects of *LDHA* overexpression and *VEGFA* knockdown on cell viability and apoptosis were evaluated. Immunoprecipitation combined with western blotting was used to detect the lactylation status of *LDHA* following OGD/R stimulation and treatment with lactic acid (LA) and 2-deoxyglucose (2-DG). Our results indicated that oxidative stress modulates *LDHA* expression, glucose uptake, and lactate production, suggesting a metabolic shift towards glycolysis. *LDHA* overexpression improved cell survival and reduced apoptosis, while *VEGFA* knockdown had the opposite effect. Additionally, 2-DG treatment reduced *LDHA* lactylation and apoptosis. Our findings demonstrated that LDHA plays a critical role in the oxidative stress response of VECs, highlighting the potential therapeutic value of targeting glycolysis in CA. This study contributes to the understanding of metabolic adaptations in vascular pathologies and suggests new avenues for therapeutic intervention in CA management.

Keywords: Cerebral aneurysms; *LDHA*; glycolysis; lactate metabolism; pathogenesis; therapeutic targets; blood vessels; enzyme; molecular mechanisms.

INTRODUCTION

Cerebral aneurysms (CA), also known as intracranial aneurysms (IA), are defined by aberrant dilatation of the cerebral arteries [1]. This vascular disease is distinguished by isolated and weak artery wall segments, which are prone to rupture and have potentially fatal effects [2]. CA are the leading cause of spontaneous subarachnoid hemorrhage (SAH), ranking third among cerebrovascular accidents behind cerebral thrombosis and hypertensive cerebral hemorrhage [3]. Its high mortality and prevalence in cardiovascular diseases have garnered significant attention. In Central and Eastern European countries, the estimated incidence of CA among adults is 3.2% [4, 5]. The multifaceted pathogenesis of cerebral aneurysms involves various factors, including genetic predisposition, hemodynamic stress, and environmental influences [6]. The mechanisms of ruptured intracranial aneurysms involve several biological processes such as inflammation, phenotypic changes in vascular smooth muscle cells (VSMC), cell adhesion, atherosclerosis, and abnormalities in extracellular matrix metabolism [7]. Current evidence suggests that abnormal inflammatory responses in the vessel wall triggered by haemodynamic changes induce the activation of signaling pathways such as NFκB by unknown mechanisms. This process leads to the production of matrix metalloproteinases (MMP), such as MMP2 and MMP9, which in turn triggers extracellular matrix degradation and phenotypic changes in VSMC, ultimately leading to aneurysm formation and rupture [8]. Inflammatory smooth muscle cells (iSMC) have been reported to induce endothelial cell (EC) dysfunction and drive the progression of intracranial aneurysms. Phoenixin-14 (PNX-14) is a newly identified brain peptide with pleiotropic effects involved in the regulation of reproduction, cardioprotection, lipid deposition, and glucose metabolism. Previous studies have shown that PNX-14 protects brain endothelial cells from oxygen-glucose deprivation/reoxygenation (OGD/R) induced cellular damage [9]. Currently,

endovascular treatments offer a viable alternative, circumventing some side effects associated with open surgery while yielding favorable outcomes [10]. Despite significant strides in comprehending molecular mechanisms, diagnostic modalities, and treatment strategies, further exploration is imperative to enhance our understanding of CA.

Lactic acid, an organic acid produced via glycolysis, serves as a key participant in cellular energy metabolism, particularly under hypoxic conditions, where glucose is metabolized into lactate, yielding limited ATP [11] . The process of lactic acid fermentation has garnered considerable attention, with scholars actively exploring its implications in various diseases, including tumors and cancers. Isoglycyrrhizin (ISL) significantly inhibited gastric cancer (GC) growth and increased apoptosis.ISL regulated the expression of proteins related to apoptosis and metabolism both in vivo and *in vitro*. ISL inhibited mitochondrial oxidative phosphorylation (OXPHOS) and glycolysis by blocking glucose uptake and inhibiting lactate production and secretion, which accompanied by increased accumulation of ROS [12]. Low DOCK8 expression induced extracellular acidification rate (ECAR) and promoted hexokinase 2 (HK-2), pyruvate kinase M2 (PKM2), and lactate dehydrogenase A (LDHA) protein expression, which in turn increased pyruvate, lactate, and ATP content. In contrast, 2-deoxy-D-glucose (2-DG) treatment was able to reverse these effects. These results suggest that DOCK8 may suppress sepsis-induced neutrophil immune function by regulating aerobic glycolysis and causing excessive inflammation [13]. Cardamonin further increased intracellular ROS levels by inhibiting the Nrf2-dependent ROS scavenging system. accumulation of ROS eventually induced apoptosis in breast cancer cells. In addition, cardamonin treatment reduced glucose uptake as well as lactate production and efflux, suggesting its important role in inhibiting glycolysis [14]. Gao R et al. revealed in their study that enhanced lactylation at the fatty acid synthase K673 site represents a downstream mechanism of

decreased liver lipid accumulation following mitochondrial pyruvate carrier 1 (MPC1) downregulation in nonalcoholic fatty liver disease (NAFLD) [15]. Gu J et al. discovered the significance of lactate as a crucial tumor metabolite, demonstrating that lactylation of MOESIN enhances the stability and function of regulatory T (Treg) cells [16]. This lactylation, in turn, promotes TGF-β signaling, facilitating tumorigenesis and proposing potential therapeutic strategies for anti-tumor immunity. In the study by Yang J et al., the inactivation of von Hippel-Lindau (VHL) in clear cell renal cell carcinoma (ccRCC) was found to trigger histone lactylation, establishing a positive feedback loop with PDGFRβ signaling that promotes ccRCC progression [17]. Correction of aberrant histone lactylation effectively inhibits ccRCC growth, and combined inhibition with PDGFRβ presents a promising therapeutic approach. Therefore, given the compelling research on lactylation in diverse diseases, the relationship between lactylation and intracranial aneurysms merits comprehensive exploration in our ongoing studies.

Cellular metabolism maintains normal cellular function by meeting its energy and metabolite requirements [18]. Human lactate dehydrogenase (LDH), which consists of two subunits, *LDHA* and *LDHB*, acts as a key glycolytic enzyme catalysing the interconversion of pyruvate and lactate in the anaerobic glycolytic pathway [19]. Although the role of *LDHB* (lactate dehydrogenase B) as a terminal metabolising enzyme in the glycolytic pathway has been extensively studied in cancer cells, relatively little research has been done on *LDHA* [20]. As a component of the lactate dehydrogenase family, *LDHA* is predominantly expressed in muscle tissues [21]. Its potential role in providing lactate molecules for lactylation modifications, influencing various cellular processes, has sparked growing interest in understanding the broader cellular functions regulated by lactate [22]. In the context of osteogenesis, Nian F et al. observed increased glucose metabolism to lactate during osteoblast differentiation, with *LDHA* playing a crucial role(23). Reduced *LDHA* levels

impair the formation of mineralized nodules and ALP activity, indicating the importance of *LDHA* in osteogenesis. Chen Y et al. demonstrated the crucial role of *LDHA* in promoting cardiomyocyte proliferation and enhancing cardiac repair post-myocardial infarction, linking it to succinyl coenzyme A reduction, Txnrd1 ubiquitination inhibition, ROS alleviation, and M2 macrophage polarization [24]. Similarly, Huo N et al. identified the STAT3/LINC00671/*LDHA* axis as a key regulatory pathway influencing glycolysis, growth, and lung metastasis in thyroid cancer [25]. Abruzzo TA et al. found in animal models that *LDHA* plays a key role in blood flow-induced dilation and remodeling of cerebral arteries, resulting in differences in susceptibility to cerebrovascular lesions in different genetic backgrounds [26]. Knockdown of *LDHA* inhibited OGD/R-induced N2a cell scotomies, and overexpression of *HMGB1* reversed this inhibition. Mechanistically, *LDHA* induces cellular focal death by targeting *HMGB1* in ischemia/reperfusion injury (CI/R) and mediating histone lactylation [27]. Expanding on this understanding, our study focused on investigating the impact of *LDHA* modulation on vascular endothelial cell proliferation and migration in brain aneurysm patients. By examining the effects of *LDHA* knockdown and overexpression on these cellular processes, we observed a promotive role of *LDHA* in cell proliferation and migration.

We sought to understand the molecular mechanism of lactate metabolism in vascular endothelial cells (VECs) under oxidative stress, with a particular emphasis on the involvement of LDHA and VEGFA in the pathogenesis of CA. Through comprehensive analysis using the GSE26969 dataset, we identified key lactate-related genes and their enriched pathways related to CA. This study focused on *LDHA* as the hub gene, and analyzed the key role of this gene in regulating oxidative stress response of VECs and its possible influence on CA progression. Furthermore, we explore the interaction between *LDHA* and *VEGFA*, two key factors in cellular stress responses and

vascular pathology. Our research emphasizes the significance of lactate metabolism and its control in cerebrovascular disorders, with the goal of shedding light on metabolic alterations in VECs during oxidative stress and identifying possible treatment targets for CA.

MATERIAL AND METHODS

The aim of the present study was to investigate ways to reveal the role of *LDHA* and *VEGFA* in oxidative stress: a pathway for therapeutic intervention in cerebral aneurysms. To this end, we performed bioinformatics analyses and designed the following series of experiments.

Download of IAs-related GSE26969 dataset and screening of differentially expressed genes (DEGs)

We retrieved the GSE26969 dataset from the Gene Expression Omnibus (GEO; https://www.ncbi.nlm.nih.gov/gds/) database [28], which included three IA samples and three normal temporal artery samples. Differential expression analysis was performed using the limma package of R software [29]. Genes with fold change (FC) > 2 were classified as up-regulated, whereas genes with FC < 0.5 were considered down-regulated, using a statistical significance threshold of $P < 0.05$.

Acquisition and enrichment analysis of lactate-related genes in GSE26969 dataset

The Gene Set Enrichment Analysis (GSEA; https://www.gsea-msigdb.org/gsea/index.jsp) website offers software tools and information to help researchers do gene set enrichment analysis, analyze genomic data, and comprehend gene expression patterns in a range of situations and disorders. In this study, we downloaded 348 lactate-related genes from this database. Then, the bioinformatics platform (https://bioinformatics.psb.ugent.be/webtools/Venn/) was used to perform intersection analysis on 384 lactate-related genes, up-regulated DEGs and down-regulated DEGs from the GSE26969 dataset to obtain overlapping genes. Functional enrichment analysis was then

performed using the Database for Annotation, Visualization, and Integrated Discovery (DAVID; https://david.ncifcrf.gov/tools) tools. Kyoto Encyclopedia of Genes and Genomes (KEGG) pathway enrichment [30], and Gene Ontology (GO) term analysis [31] covering biological processes (BP), cellular components (CC), and molecular functions (MF). When $P < 0.05$, the results were deemed statistically significant.

Construction of protein-protein interaction (PPI) network and expression analysis of key overlapping genes

Following the identification of overlapping genes, our analysis transitioned to the proteins encoded by these 63 genes. PPI networks were constructed using Cytoscape software [32]. Subsequently, the Cytohubba plugin within Cytoscape was employed, applying the Maximum Clique Centrality (MCC), Maximum Neighborhood Component (MNC), and EcCentricity algorithms to identify three key network modules. The bioinformatics platform (https://bioinformatics.psb.ugent.be/webtools/Venn/) was again used to perform intersection analysis on the genes in the three network modules to obtain key overlapping genes. Finally, the expression profiles of overlapping genes derived from the PPI network in the IA and control groups within the GSE26969 dataset were analyzed, leading to the identification of the hub gene.

Cell culture and oxidative stress induction

Shanghai Institute of Biological Sciences (Shanghai, China) provided primary vascular endothelial cells (VECs) used in this study. VECs were cultured in DMEM (Gibco, USA) supplemented with 10% fetal bovine serum (FBS) and 1% penicillin-streptomycin (Gibco, USA) in a humidified atmosphere containing 5% CO_2. Previous studies have shown that oxidative stress is a key factor in the formation and rupture of IA. To simulate oxidative stress, VECs were exposed to 0.5 mM hydrogen peroxide (H_2O_2) for 12 hours. At the same time, VECs without added H_2O_2 served as

the control group. The concentration and duration of H_2O_2 treatment were optimized in preliminary experiments to induce moderate levels of oxidative damage without causing excessive cell death [33].

Cell treatment

Subsequently, these H_2O_2-preconditioned VECs were subjected to oxygen glucose deprivation/reoxygenation (OGD/R) to simulate ischemia-reperfusion injury *in vitro*. This requires incubating cells in glucose-free DMEM under hypoxic conditions (1% O_2) for 3, 6, 12, and 24 hours, followed by reoxygenation with complete DMEM under normoxic conditions for 24 hours. Under OGD/R stimulation, VECs were simultaneously treated with 25 mM lactic acid (LA) to study the effects of acidic stress. Additionally, a separate set of VECs were treated with 2-deoxyglucose (2-DG) at a concentration of 25 mM during the reoxygenation phase to evaluate the effect of glycolysis inhibition after OGD. After OGD/R induction, both treatments were maintained for 24 hours to elucidate the cellular response to ischemic stress and the therapeutic potential of metabolic modulators in the context of endothelial cell recovery and survival [34].

Cell transfection

VECs were plated at 2×10^5 cells per well in 24-well plates to achieve optimum confluence for transfection. To regulate *LDHA* expression, VECs were transiently transfected with plasmids designed for *LDHA* overexpression (over-*LDHA*) as well as three separate small interfering RNAs (si-*LDHA*-1, si-*LDHA*-2, si-*LDHA*-3) for gene knockdown. Similarly, a *VEGFA*-specific overexpression plasmid (over-*VEGFA*) was used to overexpress *VEGFA*, whereas si-RNA targeting *VEGFA* was used to knock it down. Transfections were carried out using Lipofectamine 3000 reagent (Invitrogen, USA) according to the manufacturer's instructions.

Quantitative real-Time polymerase chain reaction (qRT-PCR) assay

Total RNA extraction from vascular endothelial cells was conducted utilizing the TRIzol reagent (Thermo Fisher Scientific, USA) according to the manufacturer's guidelines. The PrimeScript RT Reagent Kit (Takara, Japan) was employed for cDNA synthesis. Subsequent qRT-PCR assays were performed using the SYBR Green PCR Master Mix (Applied Biosystems, USA) on a StepOnePlus Real-Time PCR System (Applied Biosystems, USA). Normalization to the internal standard, glyceraldehyde-3-phosphate dehydrogenase (GAPDH) was executed [35]. The primer sequences for amplification were as follows: *LDHA* forward: 5'-ATGGCAACTCTAAGGATCA-3', *LDHA* reverse: 5'-GCAACTTGCAGTTCGGGC-3'; *VEGFA* forward: 5-CGAAAGCGCAAGAAAT-3, *VEGFA* reverse: 5- CTCCAGGGCATTAGACAGC-3. For GAPDH, the reference gene, the primers were: *GAPDH* forward: 5′-CAAGCTCATTTCCTGGTATGAC-3′, *GAPDH* reverse: 5′-CAGTGAGGGTCTCTCTCTTCCT-3′. Expression analysis utilized the $2^{-\Delta\Delta CT}$ method with GAPDH as the internal control.

Western Blotting (WB) assay

Protein lysates obtained from Vascular Endothelial Cells (VECs) were prepared using RIPA lysis buffer (Thermo Fisher Scientific, USA) supplemented with protease and phosphatase inhibitors (Thermo Fisher Scientific, USA). The BCA Protein Assay Kit (Thermo Fisher Scientific, USA) was employed to quantify protein concentrations. SDS-PAGE was utilized to separate equal protein amounts, followed by transfer to PVDF membranes (Millipore, USA). Primary antibodies targeting *LDHA* (1:100; Cell signaling Technology, Boston, USA), VEGFA (1:100; ABclonal, Wuhan, China), and GAPDH (1:5000, Cell Signaling Technology) as a loading control were used

for membrane probing. Following secondary antibody incubation, bands were visualized using ECL and captured using a ChemiDoc system.

Assessing cell viability using the cell counting kit-8 (CCK-8) assay

For the cell viability assay, VECs were seeded at a density of 5×10^3 cells per well in a 96-well plate. Following specified treatments, 10 μL of CCK-8 solution was added to each well, and cells were incubated for 1-4 hours at 37°C. The optical density was measured at 450 nm using a microplate reader, with higher absorbance indicating greater cell viability. Each experimental setup was replicated thrice to ensure consistency and statistical reliability.

Flow Cytometry

For flow cytometric analysis, detachment of VECs was achieved using trypsin-EDTA (Gibco, USA), followed by a phosphate-buffered saline (PBS) wash. Next, cells were stained using an Annexin V-FITC/propidium iodide (PI) apoptosis detection kit according to the manufacturer's instructions. Flow cytometry was conducted on a flow cytometer (BD Biosciences, USA), and FlowJo software (FlowJo LLC, USA) was employed for data analysis.

Migration assay

Twenty-four hours post-transfection, cells were harvested and resuspended at a concentration of 5×10^4 cells/well. The upper chamber of a Transwell insert (6-well format) received these cells, while the lower chamber contained complete medium as a chemoattractant. After 48 hours of incubation at 37°C, cells remaining in the upper chamber were gently removed with a cotton swab, representing non-migratory or non-invasive cells. The cells on the membrane's underside were fixed with 4% paraformaldehyde, stained with DAPI for nucleus visualization, and then counted under a fluorescence microscope to quantify migrated or invaded cells. Captured images were documented for further analysis [36].

Measurement of lactate production and extracellular acidification rate (ECAR)

VECs were treated with 0.5 mM H_2O_2 under OGD/R conditions. Glucose uptake and lactate production were assessed using a glucose uptake assay kit (Rsbio, Shanghai, China) and a lactate assay kit (Biotime, Shanghai). Concurrently, the pH of the cell medium was measured to determine changes due to metabolic activity. ECAR was measured using a Seahorse XF Analyzer (Agilent Technologies, Beijing) to track the metabolic change in VECs after H_2O_2 and OGD/R therapy. VECs were treated similarly and sequentially exposed to glucose, oligomycin A, and 2-DG to assess the glycolytic capacity and glycolytic reserve. Data were captured in real-time and plotted as ECAR against time to illustrate the cellular metabolic response to the treatments [37].

Immunoprecipitation (IP) and western blotting (WB) analysis of lactate-LDHA

Cells were lysed using ice-cold RIPA buffer supplemented with protease and phosphatase inhibitors. For immunoprecipitation, VECs treated with 0.5mM H_2O_2 were lysed, and *LDHA* was isolated using anti-LDHA antibody and Protein A/G beads. After overnight incubation, the complexes were washed and eluted for SDS-PAGE and Western blot analysis. Blots were probed with anti-lactoyllysine to detect lactylation modifications and with anti-LDHA to assess total *LDHA* levels. For assessment of dynamic lactylation after H_2O_2 treatment, VECs were incubated with 0.25mM LA and subjected to IP at intervals of 0, 8, 16, and 24 h. Additionally, cells were treated with 2-DG after OGD/R to examine the effect of glycolysis inhibition on *LDHA* lactylation [38].

Statistical analysis

The R programming language was employed for data analysis. Student's t-test assessed intergroup differences, with all data presented as mean ± SD. For comparisons across multiple groups,

Tukey's post-hoc test, in conjunction with analysis of variance (ANOVA), was applied. Statistical significance was set at $p < 0.05$ [39].

RESULTS

Functional enrichment analysis of lactate-related genes in IA

We utilized the R package to perform differential expression analysis on the GSE26969 dataset, comparing three samples of IA with three normal temporal artery samples. A total of 1725 upregulated and 1977 downregulated DEGs were identified (Figure 1A). Further performing Venn analysis on the 348 lactate-related genes in the GSEA database, as well as the up-regulated DEGs and down-regulated DEGs in the GSE26969 dataset, we identified 63 overlapping genes (Figure 1B). Subsequent functional enrichment analysis of these overlapping genes revealed significant enrichment in GO terms. In terms of BP, these genes were notably enriched in Glycolytic Process, Pyruvate Metabolic Process, Carbohydrate Catabolic Process, and others. Regarding CC term, enrichment was observed in Lysosomal Lumen, Mitochondrial Matrix, Nuclear Membrane, and others. In MF term, these genes were enriched in Lactate Dehydrogenase Activity, Oxidoreductase Activity (acting on the CH-OH group of donors, NAD or NADP as acceptor), Phosphotransferase Activity (alcohol group as acceptor), etc (Figure 1C). Furthermore, pathway analysis using the KEGG indicated significant enrichment in signaling pathways such as Glycolysis/Gluconeogenesis, Fructose and Mannose Metabolism, and Pyruvate Metabolism (Figure 1D).

Identification of key genes in IA through PPI network analysis

We extended our investigation by exploring the relationships among overlapping genes through PPI network analysis. Employing three algorithms, MCC, MNC, and EPC, we identified 10 different highly interconnected genes, respectively, revealing strong correlations within the

network (Figures 2A-2C). Among the genes exhibiting robust associations according to the different algorithms, a common set of 7 genes (*ENO2, HK1, MDH2, ALDOB, LDHA, PKLR, TALDO1*) emerged. Subsequently, we analyzed the expression profiles of these genes in the IA and normal groups in the GSE26969 dataset. It was found that *ENO2*, *HK1*, *LDHA*, and *TALDO1* were significantly less expressed in the IA group, while the other three genes (*PC*, *PGK2*, *PKLR*), on the contrary, were significantly highly expressed in the IA group (Figure 2D). Notably, our enrichment analysis unveiled the association of these genes predominantly with the lactate production process. Numerous studies have implicated lactate metabolism in the context of intracranial aneurysms. Consequently, we identified *LDHA*, a gene central to lactate production and cellular energy metabolism, as the hub gene for this study.

Effects of *LDHA* regulation on VECs proliferation and migration under oxidative stress conditions

We performed a comprehensive analysis of LDHA expression in using qRT-PCR and WB assays. Our results showed that the mRNA expression of *LDHA* was significantly reduced in VECs treated with H_2O_2 compared with the control group (Figure 3A). Consistent with the mRNA expression, WB analysis also showed that LDHA protein levels were reduced after H_2O_2 treatment (Figures 3B and 3C). Subsequently, we evaluated the transfection efficiency of VECs transfected with LDHA overexpression plasmid and *LDHA* knockdown plasmid respectively (Figures 4A-4D). Among the *LDHA* knockdown plasmids, si-*LDHA*-2 showed the most significant knockdown efficiency, so si-*LDHA*-2 was selected for subsequent knockdown experiments. Functional assays of CCK-8 and Transwell showed significant changes in cell proliferation and migration. Knockdown of *LDHA* resulted in a significant reduction in cell proliferation and migration. In contrast, *LDHA* overexpression increased cell proliferation and migration (Figures 4E and 4F).

Downregulation of *VEGFA* inhibits the protective effect of overexpressed *LDHA* on H_2O_2-induced damage to VECs

After treatment with 0.5mM H_2O_2, *VEGFA* mRNA levels were significantly upregulated in VECs compared with untreated controls, indicating that the cells responded to oxidative stress (Figure 5A). WB analysis results also showed that VEGFA protein expression increased after H_2O_2 treatment (Figures 5B and 5C). siRNA was subsequently used to knockdown *VEGFA* levels in VECs treated with 0.5mM H_2O_2, qRT-PCR and WB detection consistently detected a substantial decrease in mRNA as well as protein levels, confirming the efficiency of the gene silencing method (Figures 5D and 5E). Functional experiments showed that overexpression of *LDHA* led to increased cell viability, while knockdown of *VEGFA* reversed this result, emphasizing the critical role of VEGFA in cell survival under oxidative conditions (Figure 5F). Furthermore, when VECs were treated with H_2O_2 as assessed by flow cytometry analysis, cells overexpressing *LDHA* showed reduced apoptosis, indicating a protective effect of *LDHA*. However, co-transfection of si-*VEGFA* and *LDHA* overexpression resulted in increased apoptosis rate, suggesting that *VEGFA* knockdown may counteract the protective effects of *LDHA* overexpression (Figure 5G).

Changes in LDHA expression, glucose uptake, lactate production, and glycolytic activity in VECs under OGD/R-induced oxidative stress

WB analysis revealed that LDHA protein expression in VECs stimulated with OGD/R reduced in a time-dependent manner following exposure to 0.5mM H_2O_2, with a substantial drop detected 24 hours after treatment (Figures 6A and 6B). This implies that long-term oxidative stress can reduce LDHA protein levels. The glucose uptake test revealed that glucose absorption by VECs increased considerably during OGD/R-induced oxidative stress, indicating increased glycolytic demand (Figure 6C). Treatment with 0.5mM H_2O_2 under OGD/R conditions caused a substantial increase

in lactate generation in VECs compared to controls, indicating a shift to anaerobic metabolism (Figure 6D). Furthermore, under these conditions, the pH of the cell culture medium dropped sharply, indicating enhanced acidification due to increased lactate production (Figure 6E). Consistently, the ECAR curves exhibited dynamic metabolic adaptation following OGD/R induction, with substantial changes after adding glucose and oligomycin A, and a considerable drop after 2-DG administration, demonstrating that VECs respond to oxidative stress (Figure 6F).

LDHA overexpression and inhibition of glycolysis prevent the apoptosis of VECs cells under OGD/R-stimulated oxidative stress

When compared to untreated controls, the cell viability experiment demonstrated a substantial reduction in cell survival following OGD/R treatment. Nonetheless, under identical stress conditions, cells overexpressing *LDHA* showed a significant increase in vitality, indicating that *LDHA* protects against oxidative stress (Figure 7A). These findings were further supported by an examination of apoptosis. OGD/R markedly elevated apoptosis, and in cells overexpressing *LDHA*, apoptotic cell death was markedly enhanced (Figure 7B). Cell viability dramatically dropped when VECs were treated with 25 mM LA following H_2O_2-induced oxidative stress and OGD/R, suggesting that excess lactate exacerbates damage produced by oxidative stress (Figure 7C). Lactate is a modulator of stress-induced cell death, as demonstrated by the fact that, under OGD/R circumstances, the cell apoptosis rate was considerably greater in the LA-treated group (Figure 7D). In contrast, administration of 2-DG after OGD/R stress in H_2O_2-treated VECs resulted in a significant increase in cell viability (Figure 7E), while the apoptosis rate was significantly reduced (Figure 7F).

Regulation of LDHA lactylation in VECs under OGD/R-induced oxidative stress condition

The overall lactylation level of VECs under OGD/R-stimulated oxidative stress was assessed using IP and WB methods. The results showed that the overall lactylation level of VECs under oxidative stress was significantly enhanced under OGD/R stimulation (Figure 8A). Subsequently, a significant increase in the lactylation level of LDHA was also observed in OGD/R-stressed cells (Figure 8B). After LA treatment, the lactylation level of LDHA in cells increased in a dose-dependent manner (Figure 8C). Interestingly, the lactylation level of LDHA in OGD/R-stressed VECs cells was significantly down-regulated after 2-DG treatment (Figure 8D).

These findings of our study above revealed significant lactate-related genes and their functional enrichment in IA tissues compared to normal tissues. Through differential expression analysis, we found 63 overlapping genes enriched in metabolic processes, cellular components, and molecular functions related to glycolysis and lactate metabolism. PPI network analysis highlighted seven key genes (*ENO2*, *HK1*, *MDH2*, *ALDOB*, *LDHA*, *PKLR*, *TALDO1*) with notable expression differences between IA and normal tissues. Among these, *LDHA* emerged as a hub gene, critical for lactate production and cellular energy metabolism. Further experiments revealed that *LDHA* modulation impacts VECs proliferation and migration under oxidative stress. Specifically, *LDHA* overexpression conferred protective effects against oxidative damage, enhancing cell survival and reducing apoptosis, whereas *VEGFA* knockdown negated these benefits. Additionally, oxidative stress induced by OGD/R conditions led to altered *LDHA* expression, increased glycolysis, and lactate production in VECs. Notably, lactate modulation influenced cell viability and apoptosis, with excess lactate exacerbating oxidative damage. Finally, *LDHA* lactylation levels were significantly regulated under stress conditions, underscoring the complexity of its role in cellular stress responses. These findings underscore the pivotal role of lactate metabolism and *LDHA* in

the pathophysiology of IA and suggest potential therapeutic targets for mitigating oxidative damage in vascular endothelial cells.

DISCUSSION

CA, stemming from abnormal swelling of cerebral blood vessels, pose a severe threat to life upon rupture [40]. Stimulated inflammatory mediators release large amounts of inflammatory cytokines and oxidative factors, leading to remodelling of the phenotypic regulation and extracellular matrix (ECM) dysfunction in vascular smooth muscle cells (VSMCs). Inflammatory responses, oxidative damage and cell death are closely related to the etiology of CA [41]. Under normal physiological conditions, there is a dynamic balance between proliferation and apoptosis of VSMCs. endothelial dysfunction and phenotypic transformation of VSMCs contribute to aneurysm development [42]. And H_2O_2 is an oxidative stress inducer capable of causing apoptosis in VSMC.H_2O_2 has been used to establish an in vitro aneurysm model by inducing apoptosis in VSMC cells [43]. This model provides a useful tool for studying the underlying mechanisms and potential treatments for aneurysms. Insights from Tawk RG et al. underscore a shift from size-based approaches to comprehensive risk assessment for unruptured intracranial aneurysms (UIA) and aneurysmal subarachnoid hemorrhage (SAH) treatment, emphasizing the preferential use of endovascular coil spring in SAH therapy to improve outcomes [44]. Texakalidis P et al. comprehensively elucidate the pathobiology of CA, covering inflammatory pathways, genetics, and risk factors influencing their formation, growth, and rupture, providing a holistic overview of the biological and physical aspects underlying CA development [45]. In addition, Xu R et al. explore the effects of glycolysis and lactate-related lactation on lipid deposition, calcification, and angiogenesis in atherosclerosis as well as highlight the potential as targeted intervention pathways [46]. In our study, through functional enrichment analysis of lactate-related genes in the CA background, it was found that

these genes are involved in glycolysis process, pyruvate metabolism process, lysosomal cavity, mitochondrial matrix, lactate dehydrogenase activity, oxidoreductase Significant enrichment in activity, glycolysis/gluconeogenesis, fructose and mannose metabolism, and pyruvate metabolism. The results of our enrichment analysis showed a dependence on glycolysis, which is consistent with the results of previous studies. Elevated glycolytic activity leads to accumulation of pyruvate and its conversion to lactate in the absence of adequate oxidative phosphorylation. The acidic microenvironment created by elevated lactate levels may affect the stability and progression of CA. In addition, genes related to lysosomal and mitochondrial processes were highly enriched, suggesting that changes in organelle function may affect energy metabolism and cellular homeostasis, ultimately leading to vessel wall thinning, which is also associated with the development of aneurysms.

Lactation modification, involving acylation of lysine residues by lactate molecules, plays a pivotal role in cellular metabolism regulation [47, 48]. Given the substantial research on lactylation by various scholars, it served as a reference for our current study. Building on this knowledge, Zhang N et al. uncover the dynamic regulation of lactylation on lysine 1897 of α-myosin heavy chain (α-MHC), influencing the interaction with muscle-associated proteins and impacting cardiac structure and function [49]. The reduced lactylation of α-MHC K1897 in heart failure is attributed to diminished intracellular lactate levels, with the potential for mitigating heart failure through the modulation of this sarcomeric interaction by controlling lactate concentration. Furthermore, Fan M et al. reveal that elevated lactate levels post-myocardial infarction induce Snail1 lactylation through the TGF-β/Smad2 pathway, promoting endothelial-to-mesenchymal transition (EndoMT), leading to increased cardiac fibrosis and functional impairment, unveiling a previously unrecognized role of lactate in exacerbating adverse cardiac outcomes [50]. In gliomas, LDHA

expression was significantly elevated and positively correlated with M2 type TAM infiltration. Lactic acid secreted by glioma cells induces TAM polarisation to the M2 subtype, which in turn promotes the proliferation, migration, invasion and mesenchymal transformation of glioma cells [51]. Circ_MAPK9 promotes STAT3 and LDHA expression and influences hepatocellular carcinoma progression through silencing miR-642b-3p [52]. In our study, through bioinformatics analysis of the GSE26969 dataset comparing gene expression in CA patients and normal subjects, *LDHA* has been identified as a hub gene involved in lactate metabolism that was significantly downregulated in IA samples. Functional analysis showed that *LDHA* regulation significantly affects the proliferation and migration of vascular endothelial cells under oxidative stress, suggesting its potential role in the pathogenesis of CA.

VEGFA is a member of the PDGF/VEGF growth factor family. Studies have found that this growth factor can induce the proliferation and migration of vascular endothelial cells and is crucial for physiological and pathological angiogenesis [53, 54]. Lactate, possibly by influencing transcription factors, signaling pathway molecules, or other regulatory factors, indirectly or directly modulates the expression levels of *VEGFA* [55]. Dong SY et al. observed elevated expression of HIF-1α and its target genes, *VEGFA* and *LDHA*, in Parkinson's disease (PD) upon exposure to MPP(+), accompanied by suppressed expression of *SIRT1* [56]. This suggests a potential association between PD and the dysregulation of the *SIRT1*/*HIF-1α* signaling axis and its impact on PD pathophysiology. Additionally, Liu P et al. found a correlation between the progression of cerebral aneurysms and a decrease in smooth muscle cells (SMC) and endothelial cells (EC) within the aneurysm wall [57]. They noted an increase in matrix metalloproteinases (MMP) and a decrease in collagen levels, linked to reduced *VEGFA* expression in EC. These findings highlight potential therapeutic targets for preventing the progression of cerebral

aneurysms. Chédeville AL et al. uncovered that hypoxia-induced upregulation of *LDHA* in glioblastoma triggers a glycolytic shift [58]. This is accompanied by enhanced expression of pro-angiogenic factors, including *VEGFA*. The high expression levels of *SLC2A1*, *LDHA*, *PDK1*, *PFKFB4*, *HK2*, *VEGFA*, *SERPINE1*, *TFRC*, and *ADM* were significantly associated with overall decreased survival rates. These results underscore the potential of these factors as more effective therapeutic targets for glioblastoma. Our experimental analysis demonstrates that co-introduction of *VEGFA* into cells overexpressing *LDHA* rescues the initially observed increase in proliferation and decrease in apoptosis. This implies that there is an interaction between *VEGFA* and *LDHA* in VECs in regulating cellular responses to oxidative stress.

Upon the onset of CA, local blood circulation is compromised, leading to ischemic-hypoxic injury in the affected tissue [59]. Building on the findings of Yao X et al., who demonstrated the crucial role of lactate dehydrogenase A (*LDHA*) in brain ischemia-reperfusion (CI/R) injury, our study delved into the complex molecular landscape associated with *LDHA* in CA progression [27]. Investigating the impact of oxygen-glucose deprivation/reoxygenation (OGD/R) stimulation, Pan Q et al. discovered an upregulation of monocarboxylate transporter 4 (MCT4), induced by OGD/R, facilitating a shift towards glycolysis by regulating *LDHA* and suppressing oxidative phosphorylation (OXPHOS), ultimately contributing to cardiac protection in myocardial ischemia/reperfusion (I/R) injury [60]. Additionally, Lu B et al. revealed that reoxygenation-induced vascular endothelial cell (VEC) injury resulted in a significant reduction in the protein abundance of NR4A3, and the antioxidant steroid TRIOL countered this effect by inhibiting ROS-driven ubiquitination and degradation [61]. This highlights a novel post-translational regulation involving the interaction between NR4A3 and SMARCB1 in vascular endothelial cells. In our current investigation, we noticed a considerable increase in *LDHA* lactylation of VECs under

OGD/R-induced oxidative stress, which was further augmented by LA treatment, suggesting a dose-dependent impact. While oxidative damage is made worse by lactate buildup, overexpression of *LDHA* improves VEC recovery. It's interesting to note that 2-DG inhibits glycolysis, which lowers cell death and connects glycolytic activity to oxidative stress reactions. Under the control of 2-DG, lactoylation of *LDHA* is increased under stress, indicating a regulatory function for post-translational changes in cellular response to oxidative stress.

Our study highlighted the significant role of lactate metabolism and *LDHA* regulation in the pathogenesis of cerebral aneurysms. The findings suggest that targeting metabolic pathways, particularly glycolysis and lactate-related processes, could offer new therapeutic strategies for CA. The interplay between *LDHA* and *VEGFA* in VECs under oxidative stress further underscores the complexity of cellular responses in CA progression. Future research should continue to explore these molecular mechanisms, with an emphasis on developing targeted interventions that can mitigate oxidative damage and stabilize vascular structures, potentially improving clinical outcomes for patients with cerebral aneurysms. The strengths of this study lie in its comprehensive bioinformatics and functional analysis, providing a robust foundation for future investigations. However, the study's limitations include the need for validation in larger, diverse cohorts and the exploration of additional molecular pathways involved in CA development. The implications of this research extend beyond CA, offering insights into the broader field of vascular biology and disease.

CONCLUSION

In summary, in our comprehensive analysis, we delved into the multifaceted role of *LDHA* in CA. Particularly under oxidative stress induced by OGD/R, *LDHA* expression showed significant regulation, exerting a profound influence on cellular metabolic processes. We observed a

noteworthy correlation: *LDHA* downregulation led to increased glycolytic flux, evident through heightened glucose uptake and lactate production. This suggested a compensatory response by VECs to oxidative stress. Additionally, *LDHA* overexpression exhibited a protective role against oxidative stress-induced damage, promoting cell viability and reducing apoptosis. Notably, the downregulation of *VEGFA* reversed this protective effect. Moreover, we uncovered lactylation of *LDHA* as a pivotal post-translational modification responsive to metabolic shifts under stress conditions. This modification appeared to serve as a regulatory mechanism facilitating VECs' adaptation to oxidative stress induced by OGD/R. These findings shed light on lactate metabolism and *LDHA* regulation, deepening our understanding of cellular adaptations in CA. Furthermore, they will unveil potential therapeutic targets for mitigating disease progression in the future.

Data availability

The datasets used and/or analyzed during the current study are available from the corresponding author upon reasonable request.

REFERENCES

1. Giotta Lucifero A, Baldoncini M, Bruno N, Galzio R, Hernesniemi J, Luzzi S. Shedding the light on the natural history of intracranial aneurysms: an updated overview. Medicina. 2021;57(8):742.

2. Harrigan MR, Deveikis JP. Intracranial aneurysms and subarachnoid hemorrhage. Handbook of cerebrovascular disease and neurointerventional technique: Springer; 2024. p. 641-760.

3. Yamada Y, Kato K, Oguri M, Horibe H, Fujimaki T, Yasukochi Y, et al. Identification of nine genes as novel susceptibility loci for early-onset ischemic stroke, intracerebral hemorrhage, or subarachnoid hemorrhage. Biomedical Reports. 2018;9(1):8-20.

4. Medetov Y, Babi A, Makhambetov Y, Menlibayeva K, Bex T, Kaliyev A, et al. Risk factors for aneurysm rupture among Kazakhs: findings from a national tertiary hospital. BMC neurology. 2022;22(1):1-7.

5. Etminan N, de Sousa DA, Tiseo C, Bourcier R, Desal H, Lindgren A, et al. European Stroke Organisation (ESO) guidelines on management of unruptured intracranial aneurysms. European Stroke Journal. 2022;7(3):LXXXI-CVI.

6. Toader C, Eva L, Bratu B-G, Covache-Busuioc R-A, Costin HP, Dumitrascu D-I, et al. Intracranial Aneurysms and Genetics: An Extensive Overview of Genomic Variations, Underlying Molecular Dynamics, Inflammatory Indicators, and Forward-Looking Insights.

Brain Sciences. 2023;13(10):1454.

7. Jabbarli R, Rauschenbach L, Dinger TF, Darkwah Oppong M, Rodemerk J, Pierscianek D, et al. In the wall lies the truth: a systematic review of diagnostic markers in intracranial aneurysms. Brain Pathol. 2020;30(3):437-45.

8. Lai X-L, Deng Z-F, Zhu X-G, Chen Z-H. Apc gene suppresses intracranial aneurysm formation and rupture through inhibiting the NF-κB signaling pathway mediated inflammatory response. Bioscience Reports. 2019;39(3).

9. Ling C, Yang Y, Hu X, Cai M, Wang H, Chen C. Phoenixin-14 alleviates inflammatory smooth muscle cell-induced endothelial cell dysfunction in vitro. Cytokine. 2022;157:155973.

10. Liao L, Derelle A-L, Merlot I, Civit T, Audibert G, Tonnelet R, et al. Endovascular treatment of distal anterior cerebral artery aneurysms: long-term results. Journal of Neuroradiology. 2020;47(1):33-7.

11. Brooks GA. The science and translation of lactate shuttle theory. Cell metabolism. 2018;27(4):757-85.

12. Yu M, Pan Q, Li W, Du T, Huang F, Wu H, et al. Isoliquiritigenin inhibits gastric cancer growth through suppressing GLUT4 mediated glucose uptake and inducing PDHK1/PGC-1α mediated energy metabolic collapse. Phytomedicine. 2023;121:155045.

13. Zhu H, Xu J, Li K, Chen M, Wu Y, Zhang X, et al. DOCK8 inhibits the immune function of neutrophils in sepsis by regulating aerobic glycolysis. Immun Inflamm Dis. 2023;11(8):e965.

14. Jin J, Qiu S, Wang P, Liang X, Huang F, Wu H, et al. Cardamonin inhibits breast cancer growth by repressing HIF-1α-dependent metabolic reprogramming. J Exp Clin Cancer Res. 2019;38(1):377.

15. Gao R, Li Y, Xu Z, Zhang F, Xu J, Hu Y, et al. Mitochondrial pyruvate carrier 1 regulates fatty acid synthase lactylation and mediates treatment of nonalcoholic fatty liver disease. Hepatology. 2023:10.1097.

16. Gu J, Zhou J, Chen Q, Xu X, Gao J, Li X, et al. Tumor metabolite lactate promotes tumorigenesis by modulating MOESIN lactylation and enhancing TGF-β signaling in regulatory T cells. Cell reports. 2022;39(12).

17. Yang J, Luo L, Zhao C, Li X, Wang Z, Zeng Z, et al. A positive feedback loop between inactive VHL-triggered histone lactylation and PDGFRβ signaling drives clear cell renal cell carcinoma progression. International journal of biological sciences. 2022;18(8):3470.

18. Fan S, Wu K, Zhao M, Yuan J, Ma S, Zhu E, et al. LDHB inhibition induces mitophagy and facilitates the progression of CSFV infection. Autophagy. 2021;17(9):2305-24.

19. Drent M, Cobben NA, Henderson RF, Wouters EF, van Dieijen-Visser M. Usefulness of lactate dehydrogenase and its isoenzymes as indicators of lung damage or inflammation. Eur Respir J. 1996;9(8):1736-42.

20. Brisson L, Bański P, Sboarina M, Dethier C, Danhier P, Fontenille M-J, et al. Lactate Dehydrogenase B Controls Lysosome Activity and Autophagy in Cancer. Cancer Cell. 2016;30(3):418-31.

21. Khan AA, Allemailem KS, Alhumaydhi FA, Gowder SJ, Rahmani AH. The biochemical and clinical perspectives of lactate dehydrogenase: an enzyme of active metabolism. Endocrine, Metabolic & Immune Disorders-Drug Targets (Formerly Current Drug Targets-Immune, Endocrine & Metabolic Disorders). 2020;20(6):855-68.

22. Brooks GA. Lactate as a fulcrum of metabolism. Redox biology. 2020;35:101454.

23. Nian F, Qian Y, Xu F, Yang M, Wang H, Zhang Z. LDHA promotes osteoblast differentiation through histone lactylation. Biochemical and biophysical research communications. 2022;615:31-5.

24. Chen Y, Wu G, Li M, Hesse M, Ma Y, Chen W, et al. LDHA-mediated metabolic reprogramming promoted cardiomyocyte proliferation by alleviating ROS and inducing M2 macrophage polarization. Redox Biology. 2022;56:102446.

25. Huo N, Cong R, Sun Z-j, Li W-c, Zhu X, Xue C-y, et al. STAT3/LINC00671 axis regulates papillary thyroid tumor growth and metastasis via LDHA-mediated glycolysis. Cell death & disease. 2021;12(9):799.

26. Abruzzo TA, Kurosawa Y, Choutka O, Clark JF, Stamper DC, Martini S, et al. Genetic determinants of cerebral arterial adaptation to flow-loading. Current Neurovascular Research. 2018;15(3):175-85.

27. Yao X, Li C. Lactate dehydrogenase A mediated histone lactylation induced the pyroptosis through targeting HMGB1. Metabolic Brain Disease. 2023;38(5):1543-53.

28. Zhao J, Guo C, Ma Z, Liu H, Yang C, Li S. Identification of a novel gene expression signature associated with overall survival in patients with lung adenocarcinoma: A comprehensive analysis based on TCGA and GEO databases. Lung Cancer. 2020;149:90-6.

29. Costa-Silva J, Domingues D, Lopes FM. RNA-Seq differential expression analysis: An extended review and a software tool. PloS One. 2017;12(12):e0190152.

30. Huckvale E, Moseley HNB. kegg_pull: a software package for the RESTful access and pulling from the Kyoto Encyclopedia of Gene and Genomes. BMC Bioinformatics. 2023;24(1):78.

31. Chen L, Zhang Y-H, Wang S, Zhang Y, Huang T, Cai Y-D. Prediction and analysis of essential genes using the enrichments of gene ontology and KEGG pathways. PloS One.

2017;12(9):e0184129.

32. Soleymani F, Paquet E, Viktor H, Michalowski W, Spinello D. Protein-protein interaction prediction with deep learning: A comprehensive review. Computational and Structural Biotechnology Journal. 2022;20:5316-41.

33. Guo W, Huang D, Li S. Lycopene alleviates oxidative stress-induced cell injury in human vascular endothelial cells by encouraging the SIRT1/Nrf2/HO-1 pathway. Clin Exp Hypertens. 2023;45(1):2205051.

34. Xu S, Huang P, Yang J, Du H, Wan H, He Y. Calycosin alleviates cerebral ischemia/reperfusion injury by repressing autophagy via STAT3/FOXO3a signaling pathway. Phytomedicine. 2023;115:154845.

35. Song Z, Song H, Liu D, Yan B, Wang D, Zhang Y, et al. Overexpression of MFN2 alleviates sorafenib-induced cardiomyocyte necroptosis via the MAM-CaMKIIδ pathway in vitro and in vivo. Theranostics. 2022;12(3):1267-85.

36. Qin K, Tian G, Zhou D, Chen G. Circular RNA circ-ARFIP2 regulates proliferation, migration and invasion in human vascular smooth muscle cells via miR-338-3p-dependent modulation of KDR. Metabolic Brain Disease. 2021;36(6):1277-88.

37. Wang P, Sun J, Sun C, Zhao H, Zhang Y, Chen J. BTF3 promotes proliferation and glycolysis

in hepatocellular carcinoma by regulating GLUT1. Cancer Biol Ther. 2023;24(1):2225884.

38. Chen K, Zeng J, Sun Y, Ouyang W, Yu G, Zhou H, et al. Junction plakoglobin regulates and destabilizes HIF2α to inhibit tumorigenesis of renal cell carcinoma. Cancer Commun (Lond). 2021;41(4):316-32.

39. Luo P, Zhang Q, Zhong T-Y, Chen J-Y, Zhang J-Z, Tian Y, et al. Celastrol mitigates inflammation in sepsis by inhibiting the PKM2-dependent Warburg effect. Mil Med Res. 2022;9(1):22.

40. Frösen J, Cebral J, Robertson AM, Aoki T. Flow-induced, inflammation-mediated arterial wall remodeling in the formation and progression of intracranial aneurysms. Neurosurgical focus. 2019;47(1):E21.

41. Liu P, Song Y, Zhou Y, Liu Y, Qiu T, An Q, et al. Cyclic Mechanical Stretch Induced Smooth Muscle Cell Changes in Cerebral Aneurysm Progress by Reducing Collagen Type IV and Collagen Type VI Levels. Cellular Physiology and Biochemistry : International Journal of Experimental Cellular Physiology, Biochemistry, and Pharmacology. 2018;45(3):1051-60.

42. Chalouhi N, Ali MS, Jabbour PM, Tjoumakaris SI, Gonzalez LF, Rosenwasser RH, et al. Biology of intracranial aneurysms: role of inflammation. Journal of Cerebral Blood Flow and Metabolism : Official Journal of the International Society of Cerebral Blood Flow and Metabolism. 2012;32(9):1659-76.

43. Zhao W, Zhang H, Su J-Y. MicroRNA-29a contributes to intracranial aneurysm by regulating the mitochondrial apoptotic pathway. Molecular Medicine Reports. 2018;18(3):2945-54.

44. Tawk RG, Hasan TF, D'Souza CE, Peel JB, Freeman WD, editors. Diagnosis and treatment of unruptured intracranial aneurysms and aneurysmal subarachnoid hemorrhage. Mayo Clinic Proceedings; 2021: Elsevier.

45. Texakalidis P, Sweid A, Mouchtouris N, Peterson EC, Sioka C, Rangel-Castilla L, et al. Aneurysm formation, growth, and rupture: the biology and physics of cerebral aneurysms. World neurosurgery. 2019;130:277-84.

46. Xu R, Yuan W, Wang Z. Advances in glycolysis metabolism of atherosclerosis. Journal of Cardiovascular Translational Research. 2023;16(2):476-90.

47. Sun HL, Zhou FY, Chen DW, Tan CR, Zeng GH, Liu YH, et al. The Correlation of Tau Levels with Blood Monocyte Count in Patients with Alzheimer's Disease. J Alzheimers Dis. 2022;85(3):1321-8.

48. Chen A-N, Luo Y, Yang Y-H, Fu J-T, Geng X-M, Shi J-P, et al. Lactylation, a novel metabolic reprogramming code: current status and prospects. Frontiers in immunology. 2021;12:688910.

49. Zhang N, Zhang Y, Xu J, Wang P, Wu B, Lu S, et al. α-myosin heavy chain lactylation

maintains sarcomeric structure and function and alleviates the development of heart failure. Cell Research. 2023;33(9):679-98.

50. Fan M, Yang K, Wang X, Chen L, Gill PS, Ha T, et al. Lactate promotes endothelial-to-mesenchymal transition via Snail1 lactylation after myocardial infarction. Science Advances. 2023;9(5):eadc9465.

51. Yan C, Yang Z, Chen P, Yeh Y, Sun C, Xie T, et al. GPR65 sensing tumor-derived lactate induces HMGB1 release from TAM via the cAMP/PKA/CREB pathway to promote glioma progression. J Exp Clin Cancer Res. 2024;43(1):105.

52. Wang K, Lu Q, Luo Y, Yu G, Wang Z, Lin J, et al. Circ_MAPK9 promotes STAT3 and LDHA expression by silencing miR-642b-3p and affects the progression of hepatocellular carcinoma. Biol Direct. 2024;19(1):4.

53. Barratt SL, Flower VA, Pauling JD, Millar AB. VEGF (vascular endothelial growth factor) and fibrotic lung disease. International Journal of Molecular Sciences. 2018;19(5):1269.

54. Mesquita J, Castro-de-Sousa JP, Vaz-Pereira S, Neves A, Passarinha LA, Tomaz CT. Vascular endothelial growth factors and placenta growth factor in retinal vasculopathies: current research and future perspectives. Cytokine & growth factor reviews. 2018;39:102-15.

55. Li X, Yang Y, Zhang B, Lin X, Fu X, An Y, et al. Lactate metabolism in human health and

disease. Signal transduction and targeted therapy. 2022;7(1):305.

56. Dong S-Y, Guo Y-J, Feng Y, Cui X-X, Kuo S-H, Liu T, et al. The epigenetic regulation of HIF-1α by SIRT1 in MPP+ treated SH-SY5Y cells. Biochemical and biophysical research communications. 2016;470(2):453-9.

57. Liu P, Shi Y, Fan Z, Zhou Y, Song Y, Liu Y, et al. Inflammatory Smooth Muscle Cells Induce Endothelial Cell Alterations to Influence Cerebral Aneurysm Progression via Regulation of Integrin and VEGF Expression. Cell Transplantation. 2019;28(6):713-22.

58. Chédeville AL, Lourdusamy A, Monteiro AR, Hill R, Madureira PA. Investigating glioblastoma response to hypoxia. Biomedicines. 2020;8(9):310.

59. Shevtsova Y, Eldarov C, Starodubtseva N, Goryunov K, Chagovets V, Ionov O, et al. Identification of Metabolomic Signatures for Ischemic Hypoxic Encephalopathy Using a Neonatal Rat Model. Children. 2023;10(10):1693.

60. Pan Q, Xie X, Yuan Q. Monocarboxylate transporter 4 protects against myocardial ischemia/reperfusion injury by inducing oxidative phosphorylation/glycolysis interconversion and inhibiting oxidative stress. Clinical and Experimental Pharmacology and Physiology. 2023;50(12):954-63.

61. Lu B, Zhu Z, Sheng L, Li Y, Yang Y, Chen Y, et al. SMARCB1 promotes ubiquitination and

degradation of NR4A3 via direct interaction driven by ROS in vascular endothelial cell injury. Oxidative Medicine and Cellular Longevity. 2020;2020.

FIGURES WITH LEGENDS

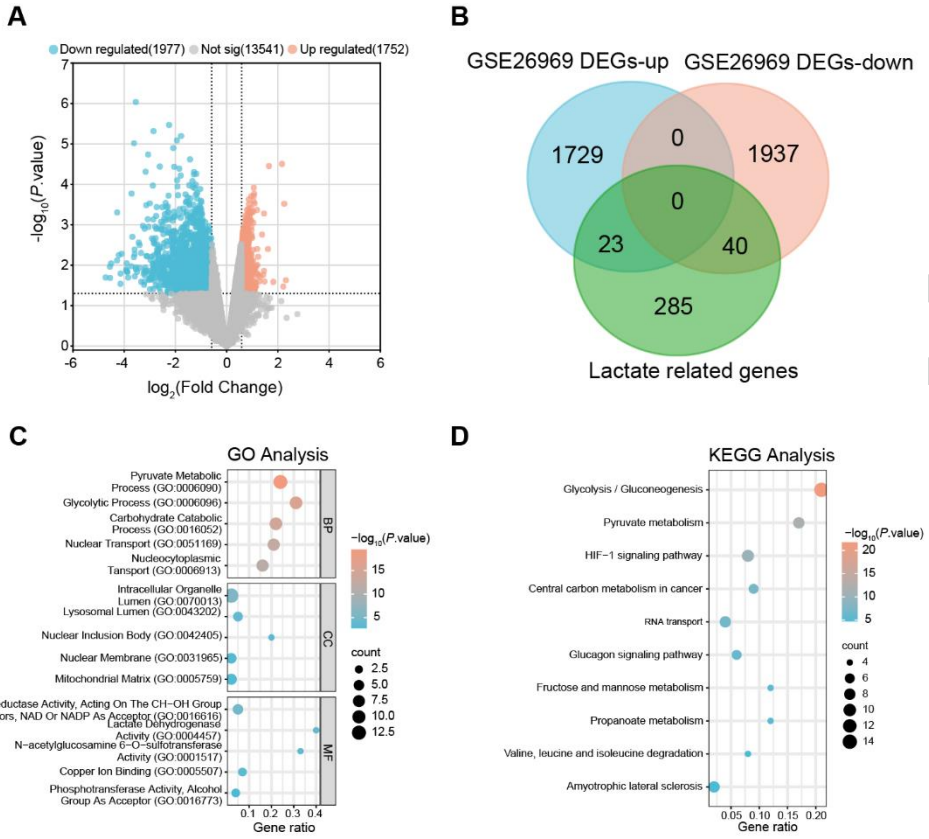

FIGURE 1. Comprehensive bioinformatics analysis of lactate-related gene expression. (A) The volcano plot visually represents the DEGs identified from the GSE26969 dataset. The X-axis (Log_2 Fold Change) signifies the logarithmic fold change in gene expression between tumor and normal samples. The Y-axis ($-log_{10}$ *p*-value) denotes the statistical significance of the observed differential expression, with higher values indicating increased significance. Each point on the plot corresponds to an individual gene, with up-regulated DEGs depicted in red and down-regulated DEGs in blue; (B) The Venn diagram illustrates the intersection of lactate-related genes with both upregulated and downregulated DEGs, providing insights into genes associated with lactation processes; (C) GO enrichment analysis delineates the functional roles of the overlapping genes, categorizing them into BP, CC, and MF. The abscissa represents GeneRatio, and the ordinate depicts the enrichment terms. Larger dots indicate a higher number of enriched genes; (D) KEGG enrichment analysis predicts the pathways in which the overlapping genes are involved, offering a comprehensive view of the biological processes associated with these genes. DEGs: Differential expressed genes; GO: Gene ontology; BP: Biological process; CC: Cell component; MF: Molecular function; KEGG: Kyoto Encyclopedia of Genes and Genomes.

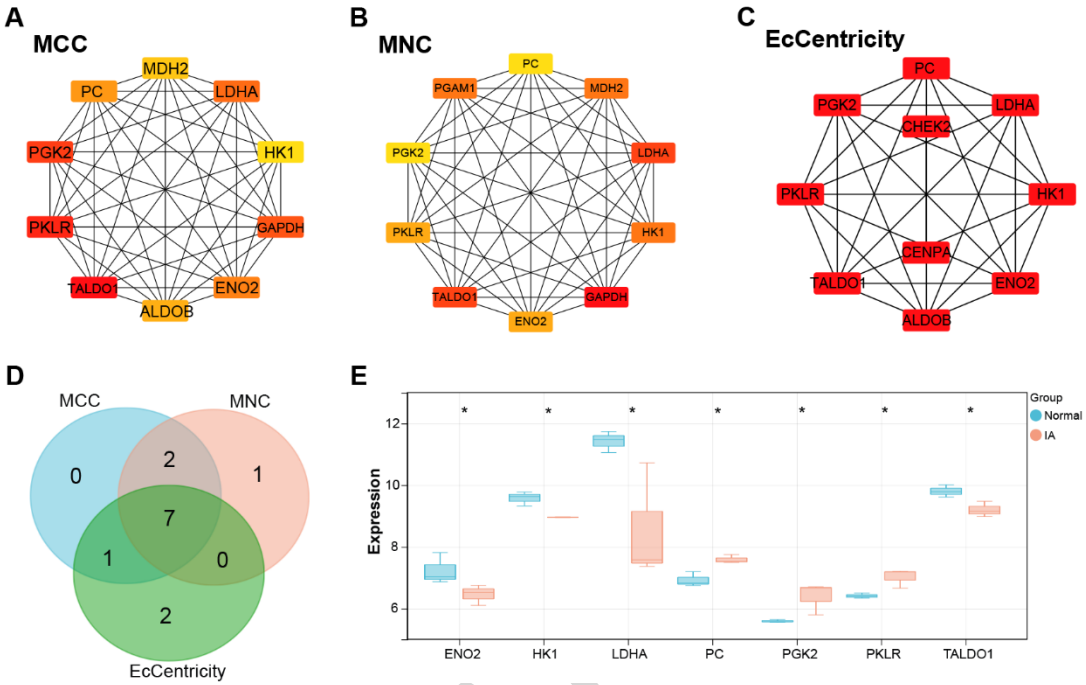

FIGURE 2. Hub genes implicate *LDHA* in IA metabolic dysregulation. (A-C) Analysis of PPI network using MCC, MNC, and EcCentricity algorithms, revealing 10 highly interconnected genes. The MCC network comprises 10 nodes and 45 edges (A); the MNC network consists of 10 nodes and 45 edges (B); the EcCentricity algorithm-derived network includes 10 nodes and 29 edges (C); (E) Boxplots depicting the expression levels of overlapping genes (*ENO2*, *HK1*, *MDH2*, *ALDOB*, *LDHA*, *PKLR*, *TALDO1*) in the IA groups and normal groups from the GSE26969 dataset. PPI: Protein-protein interaction; MCC: Maximal clique centrality; MNC: Maximum neighborhood component.

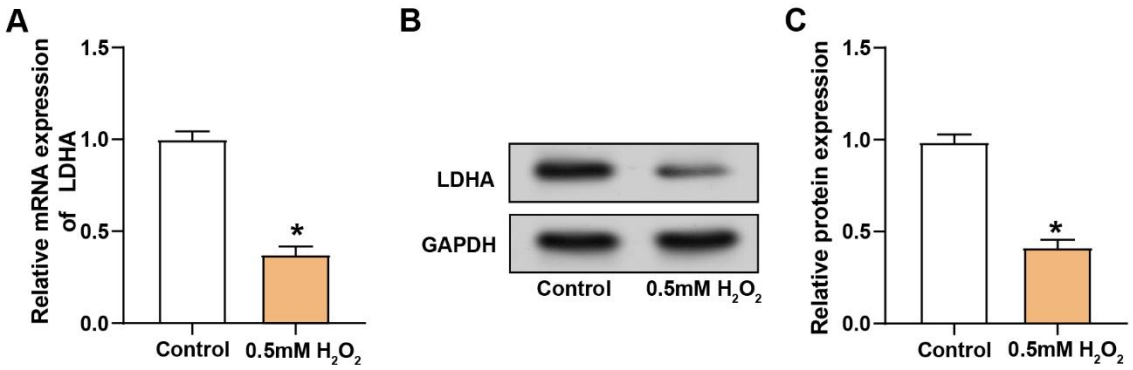

FIGURE 3. Effect of oxidative stress on *LDHA* expression in VECs. (A) Relative mRNA expression levels of *LDHA* in VECs under control conditions and after treatment with 0.5mM H_2O_2; (B) WB analysis showing LDHA protein levels in VECs under control conditions and after treatment with 0.5mM H_2O_2, using GAPDH as loading control; (C) Quantification of LDHA protein expression normalized to GAPDH demonstrating significant decrease in protein levels after H_2O_2 exposure. $^*P < 0.05$.

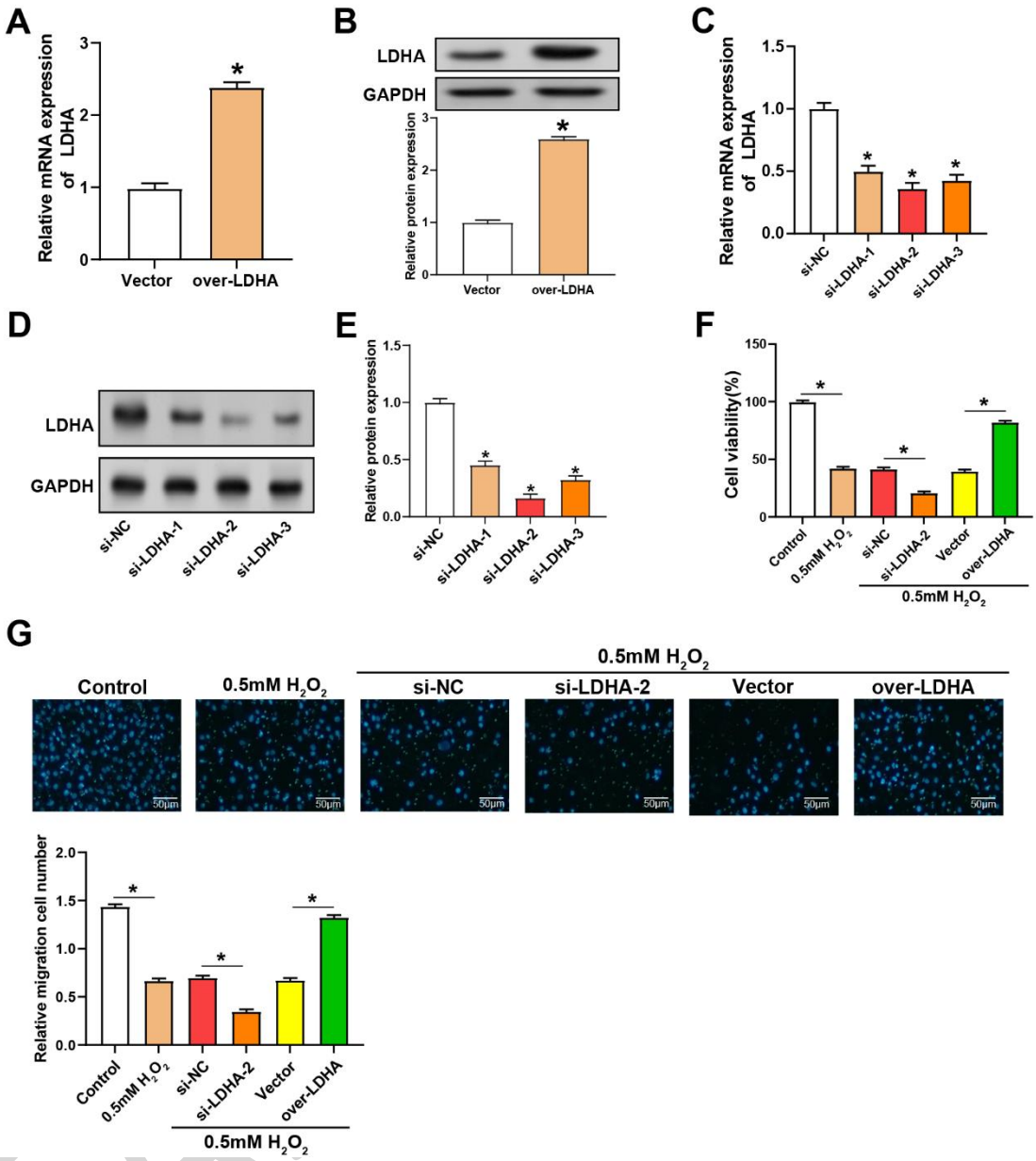

FIGURE 4. Regulation of *LDHA* affects the viability of VECs induced by H_2O_2. (A-B) qRT-PCR and WB analysis of relative mRNA expression and protein levels of LDHA in H_2O_2-treated VECs transfected with overexpression vector (over-LDHA) or control vector; (C-D) LDHA expression levels in H_2O_2-treated VECs transfected with siRNA constructs targeting LDHA (si-*LDHA*-1, si-*LDHA*-2, si-*LDHA*-3) or non-targeting control (si-NC); (E) CCK-8 assay to measure the viability of VECS treated with H_2O_2 and transfected with si-*LDHA*-2 or over-*LDHA*. The y-axis depicts the percentage of viable cells and the x-axis depicts various treatment conditions; (F) Transwell detects the migration of VECs treated with H_2O_2 under different treatments (Control, 0.5mM H_2O_2, si-NC, si-*LDHA*-2, Vector, over-*LDHA*). The six panels above

represent migrating cells, and the bar graphs are quantifications of the number of migrating cells under different treatment conditions. *$P < 0.05$.

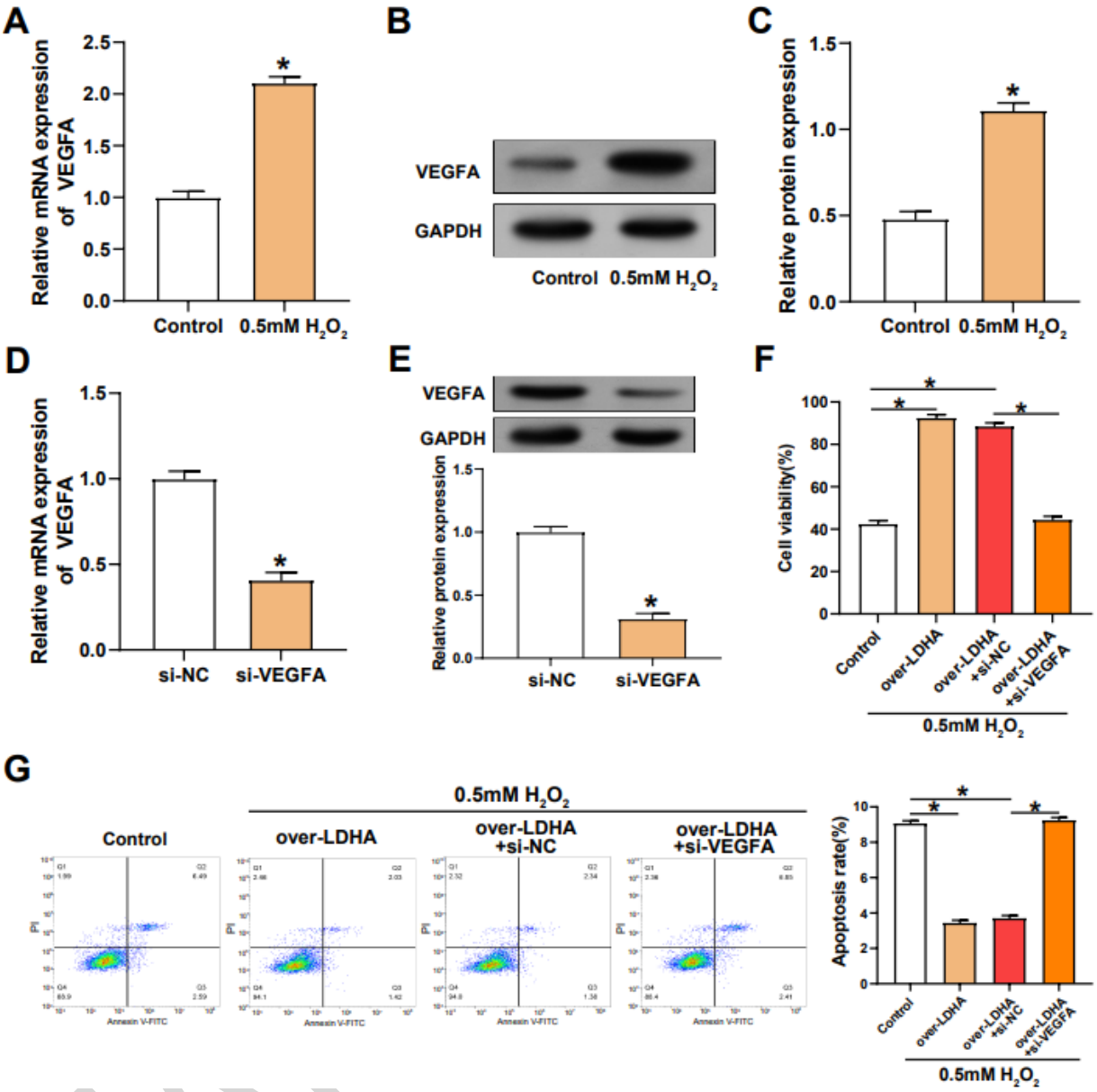

FIGURE 5. Effects of *VEGFA* and *LDHA* expression on survival and apoptosis of H_2O_2-treated VECs. (A) qRT-PCR detection of increased *VEGF*A mRNA levels in VECs after treatment with 0.5mM H_2O_2; (B) WB analysis and (C) quantitative detection showing VEGFA protein levels in VECs after 0.5mM H_2O_2 exposure; (D and E) qRT-PCR and WB detected the transfection efficiency of si-*VEGFA* in VECs treated with 0.5mM H_2O_2; (F) CCK-8 assay, the effect of *LDHA* knockdown or overexpression on cell viability in VECs after 0.5mM H_2O_2 treatment; (G) Flow cytometry apoptosis analysis shows the effect of knockdown or overexpression of *LDHA* on the apoptotic rate of VECs under oxidative stress conditions. *$P < 0.05$.

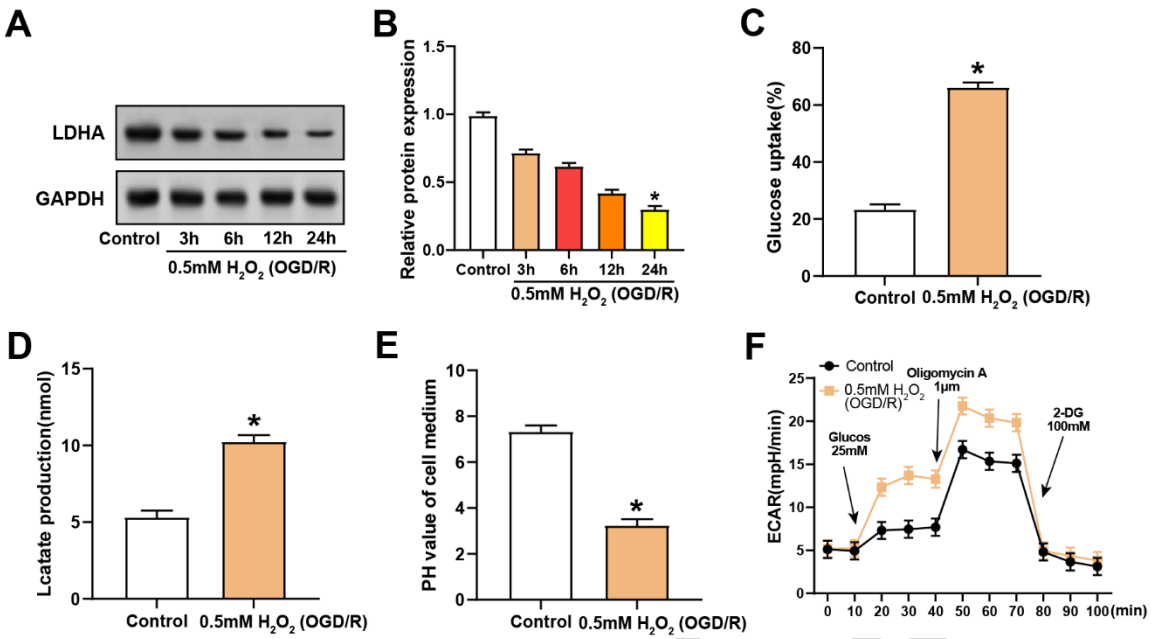

FIGURE 6. *LDHA* expression and glycolytic metabolism changes in VECs after OGD/R and H_2O_2 treatment.(A and B) WB detection of LDHA protein levels in H_2O_2-treated VECs over time after OGD/R stimulation; (C) Glucose uptake levels in H_2O_2-treated VECs after OGD/R stimulation; (D) Lactate production levels in H_2O_2-treated VECs after OGD/R stimulation; (E) PH levels in the culture medium of H_2O_2-treated VECs after OGD/R stimulation; (F) ECAR values in H_2O_2-treated VECs after OGD/R stimulation, ECAR mapping showing results after Glucos (25 mM), Oligomycin A (1 μM), and 2-DG (100 mM) injection. *$P < 0.05$.

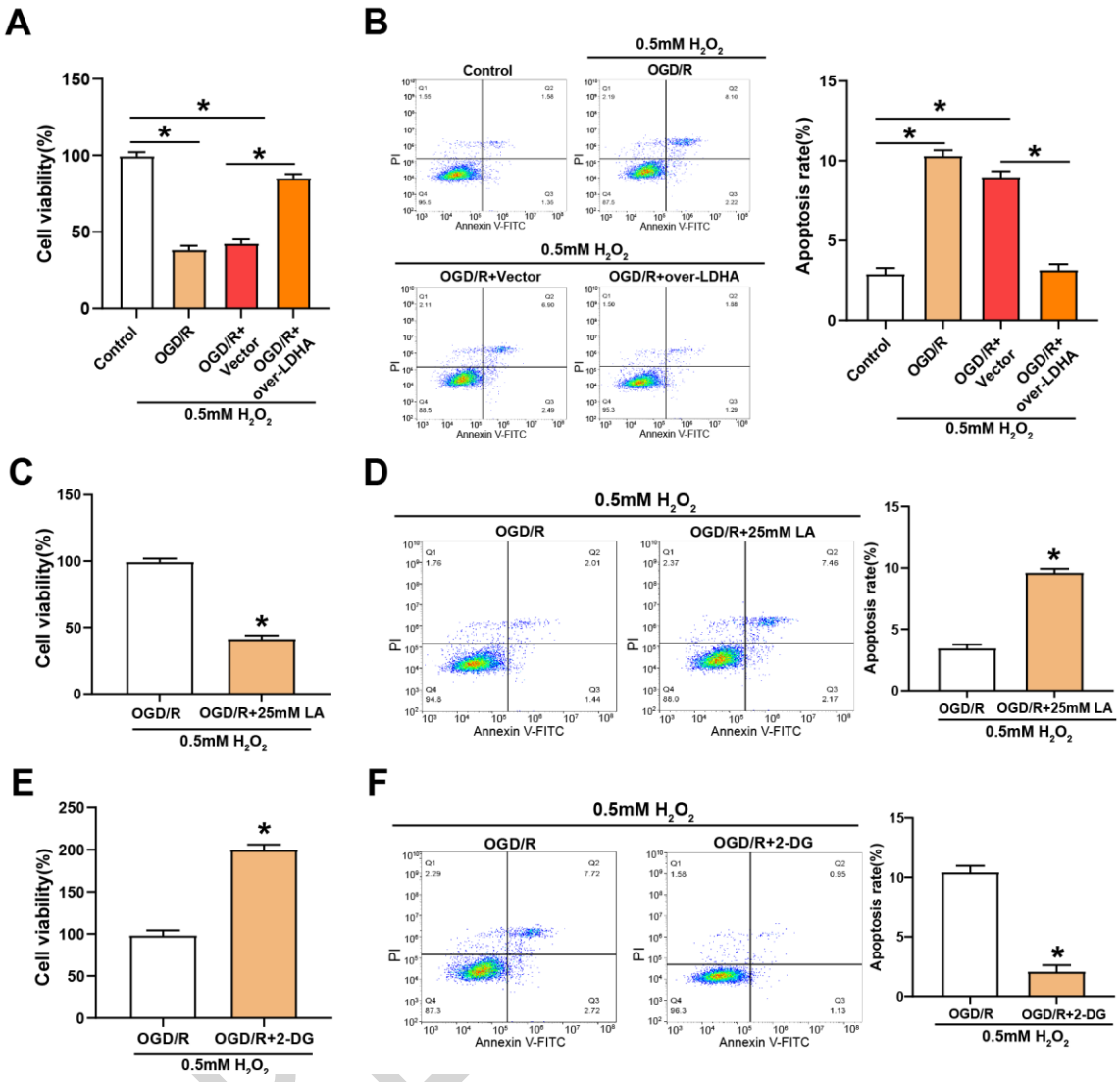

FIGURE 7. Modulation of cellular proliferation and apoptosis in H_2O_2-treated VECs under OGD/R stress and *LDHA* overexpression. (A) CCK-8 assay of cell viability of VECs treated with 0.5mM H_2O_2 under OGD/R stimulation with/without *LDHA* overexpression. The y-axis represents the percentage of viable cells, and the x-axis represents different treatment conditions; (B) Flow cytometry analysis of the apoptosis rate of VECs treated with 0.5mM H2O2 in different groups (OGD/R, OGD/R +Vector, OGD/R +over-LDHA). The x-axis represents fluorescence intensity, the y-axis represents cell count, and the bar graph illustrates the apoptotic rate; (C and D) CCK-8 assay (C) and flow cytometry (D) evaluating proliferation and apoptosis of H_2O_2-treated VECs under OGD/R treatment with the addition of 25 mM LA; (E and F) CCK-8 assay (E) and flow cytometry (F) assessing proliferation and apoptosis of H_2O_2-treated VECs under OGD/R treatment with the addition of 2-DG. *$P < 0.05$.

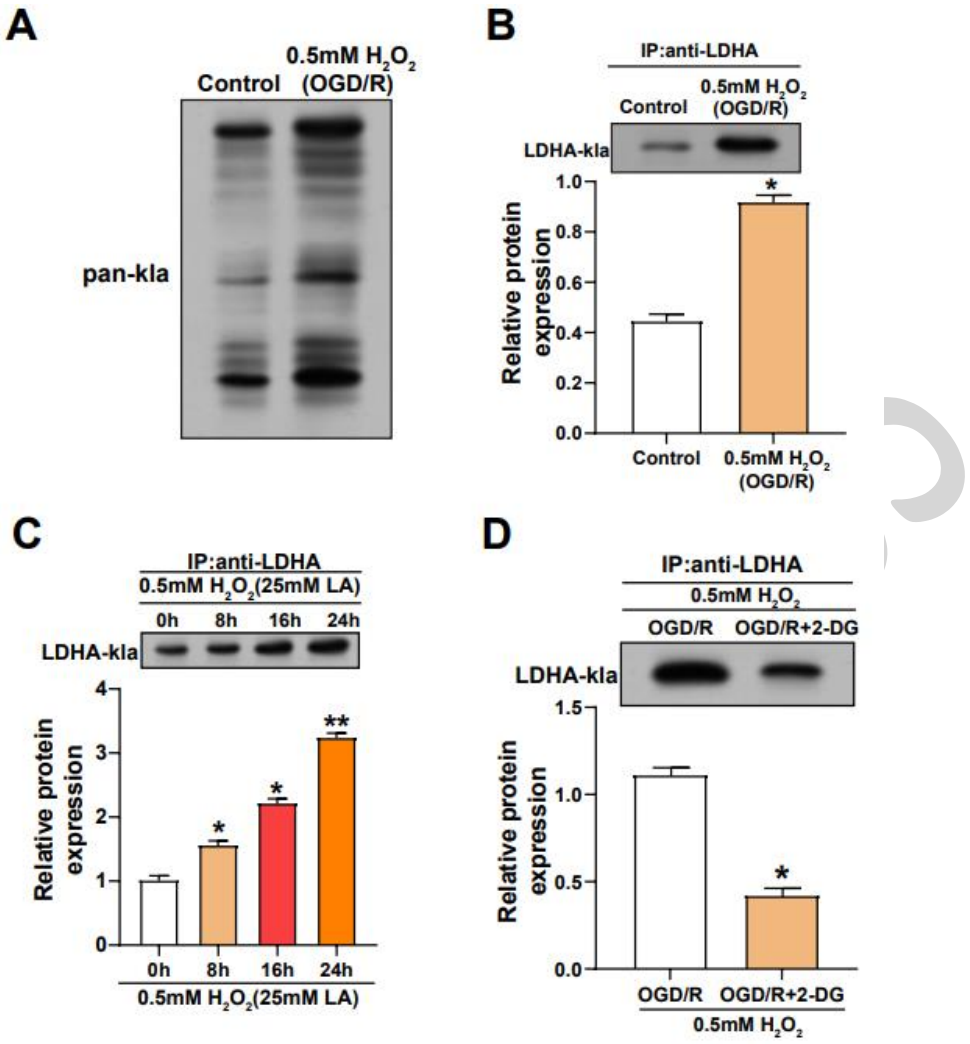

FIGURE 8. Modulation of LDHA lactation levels by OGD/R stimulation. (A) IP and WB assays detected the overall lactation level of H_2O_2-treated VECs stimulated by OGD/R; (B) The lactation level of LDHA in H2O2-treated VECs stimulated by OGD/R was detected by IP and WB assay; (C) IP and WB assays were performed to detect the lactation level of LDHA in H2O2-treated VECs treated with 25mM LA for different times; (D) IP and WB assays were performed to detect the lactation level of LDHA in H_2O_2-treated VECs stimulated by OGD/R and 2-DG. *$P < 0.05$; **$P < 0.01$.

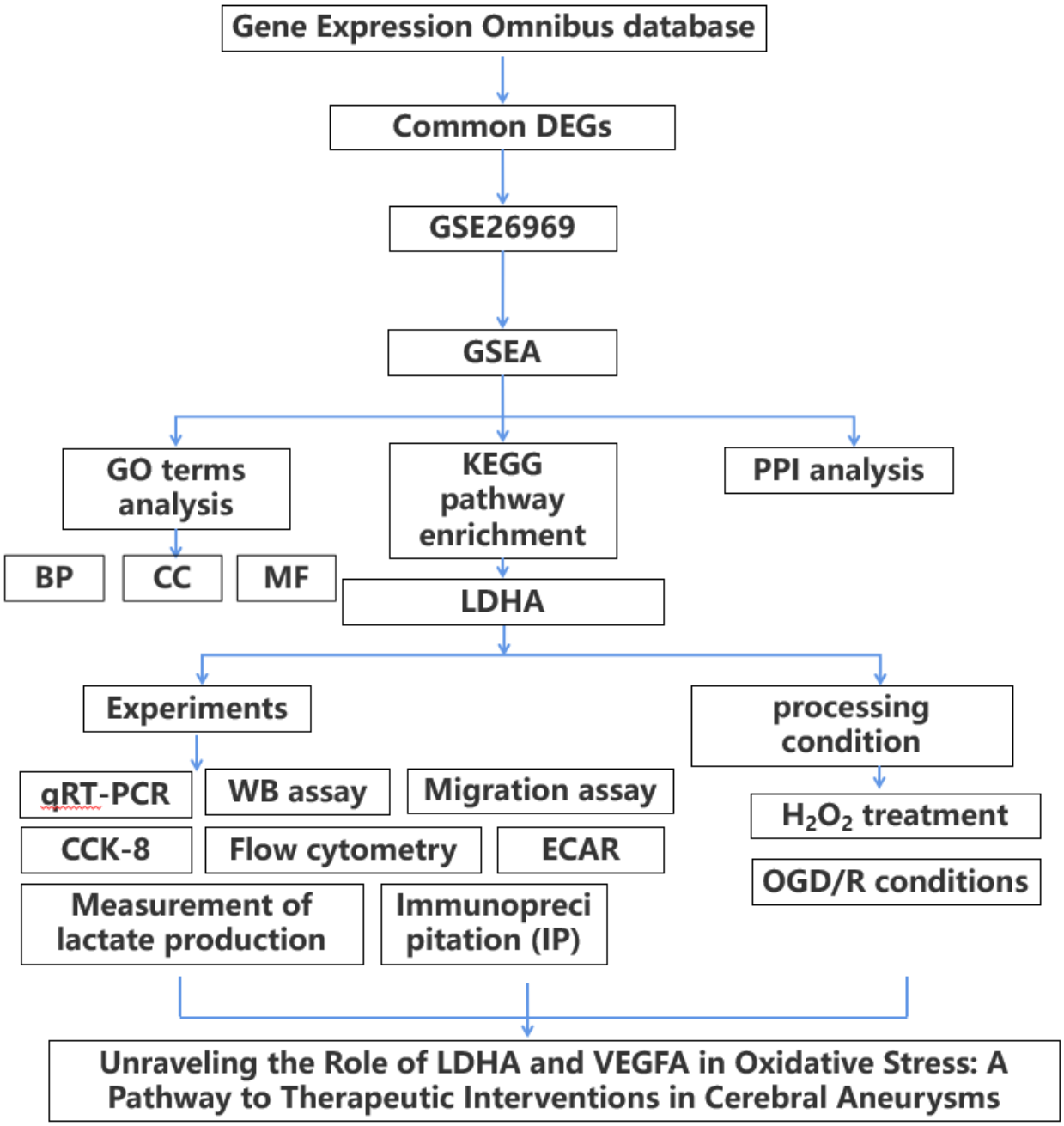

FIGURE. Graphical abstract